chemistry

MDPI

Article

2,4,6-Trichlorophenyl-Substituted [3]Triangulene with Enhanced Stability

Yiming Yang, Peipei Liu, Xiaoli Zhao * and Xueliang Shi *

Shanghai Key Laboratory of Green Chemistry and Chemical Processes, State Key Laboratory of Petroleum Molecular & Process Engineering, School of Chemistry and Molecular Engineering, East China Normal University, Shanghai 200062, China

* Correspondence: xlzhao@chem.ecnu.edu.cn (X.Z.); xlshi@chem.ecnu.edu.cn (X.S.)

Abstract: Triangulene, also known as Clar's hydrocarbon, has been sought after by chemists for more than 70 years but with limited success. Herein, we report an oxidative dehydrogenation method to synthesize two kinetically blocked [3]triangulene derivatives **TRI-1** (reported) and **TRI-2** (newly synthesized), in which the three most reactive sites are substituted by bulky mesityl groups and electron-withdrawing 2,4,6-trichlorophenyl groups, and meanwhile, three vertices of triangulene are substituted by tert-butyl groups. Interestingly, the dihydro-triangulene core possesses two isomers well characterized by UV-vis, NMR spectroscopy, and X-ray crystallographic analysis, which is interestingly substituent-dependent. The newly synthesized **TRI-2** is isolated in crystalline form, and X-ray crystallographic analysis reveals that the aryl substituents are nearly perpendicular to the triangulene plane and thus cause little perturbation of the electronic properties of the triangulene. Notably, 2,4,6-trichlorophenyl-substituted **TRI-2** exhibits enhanced stability compared to the reported mesityl-substituted **TRI-1**, e.g., **TRI-2** is stable for months in a crystalline state under a nitrogen atmosphere, and **TRI-2** in a solution state is also more persistent than **TRI-1** (half-life for **TRI-1** ≈ 18 h vs. **TRI-2** ≈ 132 h). This achievement will facilitate the design and synthesis of stable triangulene dimers and oligomers with higher spin multiplicity.

Keywords: Clar's hydrocarbon; non-Kekulé structure; triangulene; persistent radical; organic magnetic materials

check for updates

Academic Editors: Takashi Kubo, Yasutaka Kitagawa and Manabu Abe

Received: 24 February 2025
Revised: 10 March 2025
Accepted: 10 March 2025
Published: 13 March 2025

Citation: Yang, Y.; Liu, P.; Zhao, X.; Shi, X. 2,4,6-Trichlorophenyl-Substituted [3]Triangulene with Enhanced Stability. *Chemistry* **2025**, *7*, 39. https://doi.org/10.3390/chemistry7020039

Copyright: © 2025 by the authors. Licensee MDPI, Basel, Switzerland. This article is an open access article distributed under the terms and conditions of the Creative Commons Attribution (CC BY) license (https://creativecommons.org/licenses/by/4.0/).

1. Introduction

Graphene fragments with triangular shapes ([n]triangulenes) [1–4], characterized by three zigzag edges [5–7], naturally host one or more unpaired electrons, resulting in a high-spin ground state by default [8–14]. These molecules have garnered significant attention in recent years due to their potential applications in high-spin organic ferromagnets, spintronics, molecular electronics, and catalysis, as well as their importance in fundamental research [15–20]. Despite these interests, the synthetic chemistry of [n]triangulenes remains both a resurgent focus and a persistent challenge since Eric Clar's pioneering efforts to synthesize [3]triangulenes in the 1950s [21–23]. The inherent instability caused by their unpaired electrons complicates their synthesis and isolation, as these species are highly reactive [24–32]. For instance, the spin density in [3]triangulene is predominantly concentrated along the zigzag edges (Figure 1a, α- and γ-positions), which significantly contributes to its reactivity [33]. Consequently, both pristine and (partially) substituted forms of [3]triangulenes are susceptible to oxidation, dimerization, and polymerization [11,32–35].

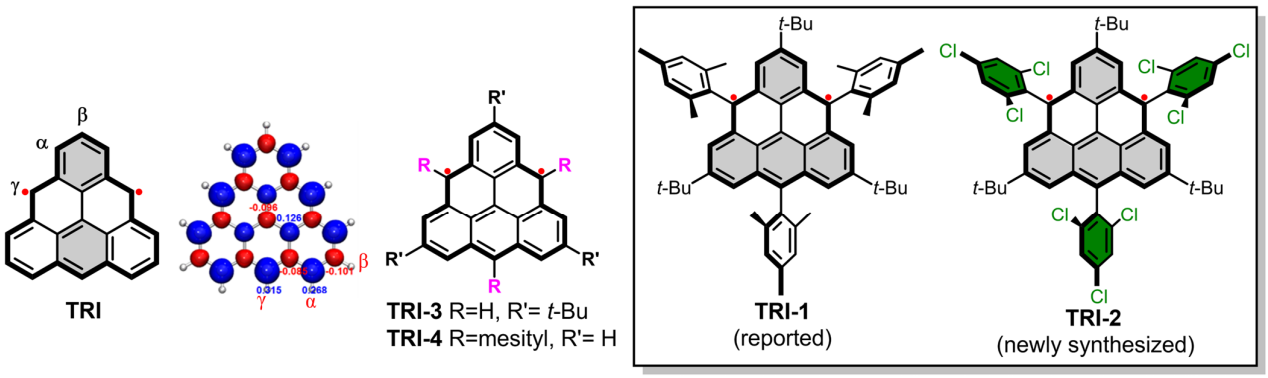


Figure 1. (**a**) Molecular structure and spin density of [3]triangulene. (**b**) [3]triangulene with different substituents (**TRI-3** and **TRI-4**). (**c**) Molecular structures of **TRI-1** (reported) and **TRI-2** (newly synthesized).

Many attempts have been made in the synthesis, isolation, and characterization of [3]triangulene derivatives with triplet ground states. The first successful observation of [3]triangulene (**TRI**) as a single molecule was made by Pavliček et al., who used STM and AFM techniques on Cu(111) surfaces under ultrahigh-vacuum conditions at 5 K [12]. To enhance stability, Nakasuji et al. designed **TRI-3** by introducing three tert-butyl groups at the β-positions, which are less reactive compared to the parent **TRI** (Figure 1b) [36]. This confirmed the triplet ground state of [3]triangulene experimentally for the first time, while **TRI-3** was found to be highly reactive and could not be isolated. The lack of steric protection at the γ-positions, where significant spin density resides, leads to the polymerization of **TRI-3** at room temperature, hindering further stabilization. Additionally, Michal Juríček et al. synthesized the persistent triangulene **TRI-4** by introducing three mesityl groups at the γ-positions, with its EPR signal detectable even after 3 weeks in a nitrogen atmosphere (Figure 1b) [37]. However, the crystallization of **TRI-4** was unsuccessful. In 2021, Shimizu et al. successfully isolated **TRI-1** in crystalline form for the first time, marking the first instance of stable triangulene being synthesized, isolated, and well characterized via wet chemistry [38]. Nevertheless, stability has consistently been a critical prerequisite for the construction of high-order triangulene fragments and the investigation of their electronic and spintronic applications.

Herein, we describe the synthesis and isolation of kinetically stabilized triangulene derivatives **TRI-1** and **TRI-2**, in which the newly synthesized **TRI-2** is isolated in a crystalline form (Figure 1c). The key to success lies in the incorporation of three tert-butyl groups at the β-positions and the introduction of three bulky and electron-withdrawing 2,4,6-trichlorophenyl groups onto the γ-positions. Interestingly, the dihydro-triangulene (**αH-TRI**) is found to have two isomers and is substituent-dependent, after being thoroughly investigated by UV-vis spectroscopy, NMR spectroscopy, and X-ray crystallographic analysis. Notably, compared with **TRI-1**, the newly synthesized **TRI-2** shows enhanced stability. It is stable for months in a crystalline state and its solution is also more persistent than **TRI-1** at room temperature in the dark under a nitrogen atmosphere. This work will pave the way for the development of various triangulene dimers and oligomers and other high-spin systems with enhanced stability.

2. Materials and Methods

All reagents and starting materials (purity ≥ 98%) were obtained from commercial suppliers (Energy Chemical, Shanghai, China) and used without further purification. All air-sensitive reactions were carried out under an inert N_2 atmosphere. All chemical agents

and solvents, unless otherwise stated, were purchased from commercial suppliers (Energy Chemical, Shanghai, China) and used directly without further purification. Tetrahydrofuran (THF) and toluene were distilled before use. Column chromatography was performed with silica gel (200–300 mesh).

We also used a Bruker 400 MHz nuclear magnetic resonance (NMR) spectrometer (Bruker, Beijing, China), IKA RET basic magnetic heating stirrer (IKA, Shanghai, China), IKA RV 10 rotary evaporator (IKA, Shanghai, China), Shimadzu UV2700 UV-Vis spectrophotometer (Shimadzu, Shanghai, China), America Thermo Fisher LTQ ESI-MS (Thermo Fisher, Shanghai, China), and a Bruker EMX instrument EMXPLUS-10/12 EPR (Bruker, Shanghai, China).

^{1}H NMR and ^{13}C NMR spectra were recorded on a Bruker 400 MHz NMR spectrometer at room temperature. $CDCl_3$ and CD_2Cl_2 were used as a field-frequency lock, and the chemical shifts were reported in δ relative to a teramethylsilane (TMS) internal standard (δ = 0).

Stability was recorded on a Shimadzu UV2700 UV-Vis spectrophotometer at room temperature. The half-life time of **TRI-2** was detected by the decay of the absorption peak at 415 nm. Solutions of **TRI-1** and **TRI-2** were prepared at a concentration of 2×10^{-5} mol/L in DCM.

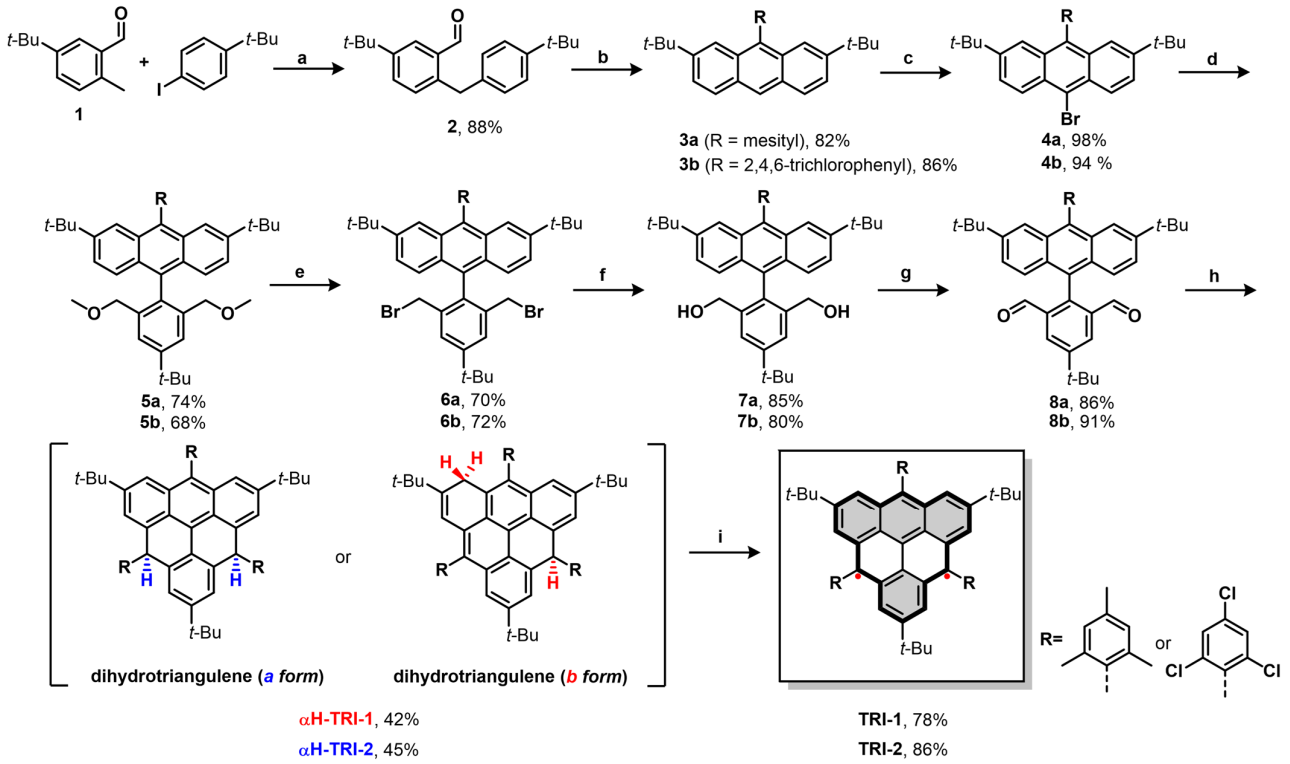
Cyclic voltammetry (CV) was recorded on a Bio-Logic SAS SP-150 spectrometer (Shanghai, China) in dichloromethane containing n-Bu_4NBF_4 (0.1 M) as a supporting electrolyte at a scan rate of 20 mV/s at room temperature. The CV cell has a glassy carbon electrode, a Pt wire counter electrode, and a Ag/Ag+ reference electrode. The potential was calibrated against the ferrocenium/ferrocene (Fc^+/Fc) couple.

The EPR spectra of **TRI-1** and **TRI-2** were recorded on a Bruker EMX instrument EMXPLUS-10/12 at room temperature. Solutions of **TRI-1** and **TRI-2** were prepared at a concentration of 0.5 mM toluene at 298 K in the dark under a nitrogen atmosphere.

3. Results

3.1. Design and Synthesis

We started the synthesis of compounds **TRI-1** and **TRI-2** from the substrates **1** and 4-tert-butyliodobenzene, which contain two tert-butyl groups (Scheme 1). These compounds enable the positioning of the tert-butyl group at the β-position of the triangulene. Substrate **2** was first synthesized via carbon–hydrogen bond activation [39]. Next, the mesityl- and trichlorophenyl-substituted **3a** and **3b** were obtained via nucleophilic addition, cyclization, and oxidative dehydrogenation reactions. Subsequently, **4a** and **4b** were obtained in high yield through the bromination of **3a** and **3b**, respectively. The dialdehyde intermediates **8a** and **8b** were prepared in four steps from **4a** and **4b**, including a Suzuki cross-coupling reaction, substitution of the methoxy groups with bromide, substitution of bromides with acetate, ester hydrolysis, and Swern oxidation [40]. Treatment of **8a** with mesitylmagnesium bromide generated the diol intermediate, which subsequently underwent Friedel–Crafts alkylation, mediated by $BF_3{\cdot}Et_2O$, which afforded the dihydrotriangulene **αH-TRI-1**. The synthesis of **αH-TRI-2** followed a similar procedure, with 2,4,6-trichlorophenyl groups being introduced at the γ-positions of the triangulene. Oxidative dehydrogenation of the dihydro-triangulene precursors **αH-TRI-1** and **αH-TRI-2** with DDQ in toluene at room temperature gave the desired products **TRI-1** and **TRI-2** both as dark-yellow solids in high yield. **TRI-1** and **TRI-2** are sensitive to silica gel (even after deactivation with trimethylamine) but can be purified by a Bio-beads column followed by recrystallization from a toluene/n-hexane mixed solvent system (see Figure S1).



Scheme 1. The synthesis of **TRI-1** and **TRI-2**: (a) AgTFA, $Pd(OAc)_2$, glycine, AcOH:H_2O = 10:1, 100 °C, 12 h; (b) (i) mesitylmagnesium bromide or (2,4,6-trichlorophenyl)magnesium iodide, THF, 0 °C, 12 h; (ii) $BF_3{\cdot}Et_2O$, DCM, r.t., 5 h; (iii) DDQ, DCM, r.t., 5 h; (c) NBS, chloroform, r.t., 1 h; (d) $Pd(PPh_3)_4$, (4-(tert-butyl)-2,6-bis(methoxymethyl)phenyl)-boronic acid, K_2CO_3, toluene/H_2O = 10:1, 110 °C, 24 h; (e) HBr, DCM, r.t., 12 h; (f) (i) AcOK, tetrabutylammonium bromide (TBAB), DMF, 100 °C, 16 h; (ii) KOH, THF, H_2O, EtOH, 80 °C, 6 h; (g) $(COCl)_2$, DMSO, NEt_3, DCM, −78 °C to 0 °C, 12 h; (h) (i) mesitylmagnesium bromide or (2,4,6-trichlorophenyl)magnesium iodide, THF, 0 °C, 12 h; (ii) $BF_3{\cdot}Et_2O$, DCM, r.t., 5 h; (i) DDQ, toluene, r.t., 8 h.

3.2. Structural Characterization of Two Dihydro-Triangulene Isomers

A previous study by Juríček et al. showed that the dihydro-triangulene precursor possessed two isomers, i.e., the *a* form, where the two hydrogen atoms are located at the γ-carbons, and the *b* form, wherein a rearrangement occurs and the hydrogen atoms are positioned at the α-carbons [37]. Interestingly, in contrast to the previous report, the mesityl-substituted dihydro-triangulene **αH-TRI-1** was found to exist as a sole *b*-form isomer (Figure 2a). Specifically, in contrast to the complicated NMR spectrum showing two sets of signals corresponding to a mixture of two isomers reported by Juríček et al., the NMR spectrum of **αH-TRI-1** displayed a set of distinct and well-resolved peaks, including the methylene protons of the α-carbon, which could be assigned to a single *b*-form isomer (Figure 2d). In addition, as shown in Figure 2e, the UV-vis absorption spectra of **αH-TRI-1** exhibited the characteristic absorption peaks of the *b* form (300–350 nm), without the finger peaks of the anthracene fragment (400–500 nm). Finally, the structure of **αH-TRI-1** was unambiguously confirmed by X-ray crystallographic analysis, clearly revealing the presence of two methylene groups at the α-carbon positions (red color) (Figures 2c and Figure S2). More interestingly, when the γ-positions were substituted with 2,4,6-trichlorophenyl groups, the dihydro-triangulene **αH-TRI-2** existed as an *a*-form isomer, which was also well characterized (Figure 2b). In particular, the NMR spectrum of **αH-TRI-2** exhibited high symmetry in the aromatic region, with distinct peaks corresponding to seven types of hydrogen and the absence of the hydrogen of the methylene group at the α-positions (Figure 2d). In addition, the UV-vis absorption of **αH-TRI-2** showed the characteristic

vibronic progression of anthracene subunits, indicating that the electronic structure of the *a* form was preserved (Figure 2e). Eventually, the structure of **αH-TRI-2** was unequivocally confirmed by X-ray crystallographic analysis, wherein two hydrogen atoms were located at the γ-carbon position of the triangulene fragment (blue color) (Figure 2f). This interesting substituent-dependent isomerization may be ascribed to the distinct electron-rich and electron-deficient nature of two substituents. The mesityl-substituted *a*-form isomer may be vulnerable to oxidation due to the electron-rich character of the mesityl groups, facilitating the rearrangement during the ring closure process to generate the *b* form. By contrast, the electron-deficient substituent 2,4,6-trichlorophenyl could stabilize the *a*-form isomer of the dihydro-triangulene precursor.

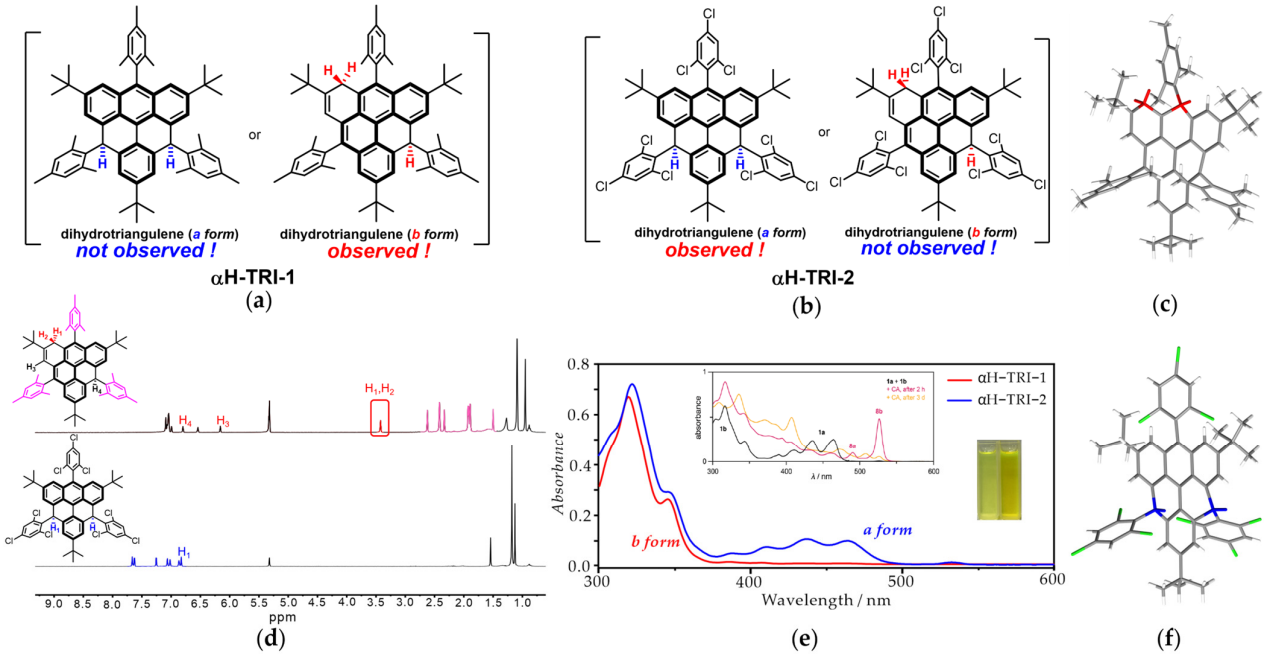


Figure 2. The isomer of **αH-TRI-1** (**a**) and **αH-TRI-2** (**b**). The X-ray crystallography results of **αH-TRI-1** (**c**) and **αH-TRI-2** (**f**). (**d**) Top: ^{1}H NMR spectrum of **αH-TRI-1** (400 MHz, CD_2Cl_2, 298 K) (insert: the structure of **αH-TRI-1**; red frame: the peak of hydrogen at the α-position; pink peak: the hydrogen of the methyl group in mesitylene). Bottom: ^{1}H NMR spectrum of **αH-TRI-2** (400 MHz, CD_2Cl_2, 298 K) (insert: the structure of **αH-TRI-2**; blue peak: the hydrogen of the triangulene framework and trichlorophenyl groups). (**e**) The UV-vis absorption spectrum of **αH-TRI-1** (red) and **αH-TRI-2** (blue) in dichloromethane (2×10^{-5} M) at 298K (insert: the UV-vis absorption spectrum of the *a* form and *b* form (black line) of dihydro-triangulene reported by Juríček et al. [37], the photographs of **αH-TRI-1** (left cuvette) and **αH-TRI-2** (right cuvette) solutions in dichloromethane (2×10^{-5} M)).

*3.3. Optical and Structural Characterization of **TRI-1** and **TRI-2***

The oxidation processes of both **αH-TRI-1** and **αH-TRI-2** were monitored over time using UV-vis spectroscopy to track the changes in their absorption characteristics (Figure S1). The results were consistent with the reported work by Juríček et al. that the precise addition of the oxidizing agent enabled a stepwise oxidation process, first forming a mixture of monoradical species, followed by the formation of **TRI-1** and **TRI-2** [37] (for more detail, see Figure S1). Consistent with the reports by Shimizu et al. and Juríček et al., the UV-vis absorption spectra of **TRI-1** and **TRI-2** exhibit three distinct groups of absorption peaks, occurring at 324–332 nm, 415 nm, and 484–515 nm (Figure S1) [38]. **TRI-1** and **TRI-2** exhibited sufficient stability to be handled outside the glovebox using deoxygenated solvents and standard Schlenk techniques. The isolation of **TRI-2** in crystalline form was achieved by the slow evaporation of a toluene/n-hexane solution in an H-tube (Figure 3a). A

comparison of the crystals of the dihydro-triangulene **αH-TRI-2** and **TRI-2** revealed that the triangulene framework in **TRI-2** exhibited enhanced planarity (Figures 3b and Figure S3). In addition, the structure of **TRI-2** displayed a high degree of symmetry, and the hybridization of the γ-carbon atom in **αH-TRI-2** changed from sp^3 to sp^2. Moreover, a comparison of the bond length alteration between **TRI-2** and **αH-TRI-2** revealed a significantly more uniform bond length in **TRI-2** (Figure 3c,d). These findings provide strong evidence that the dihydro-triangulene precursor undergoes complete oxidative dehydrogenation to form triangulene **TRI-2**. Owing to the bulky substitution, intermolecular π-π stacking is absent between the triangulene cores, with molecular packing primarily driven by multiple [C-H· · · π] and [C-H· · · Cl] interactions (Figure S5).

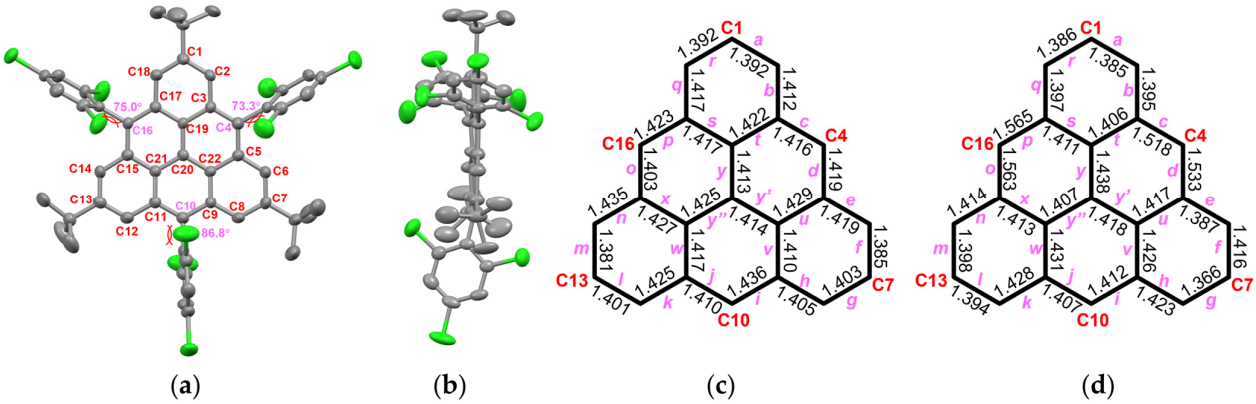


Figure 3. X-ray crystallographic structure of **TRI-2** in top view (**a**) and side view (**b**). The bond length (Å) of the triangulene backbone for **TRI-2** (**c**) and **αH-TRI-2** (**d**) with labeling.

3.4. EPR and Stability Measurements

The magnetic properties of **TRI-1** and **TRI-2** in toluene were characterized using EPR spectroscopy (Figures 4a and Figure S6). In accordance with the report by Shimizu et al., both spectra exhibited a width of 3.3 mT and were split into a septet by six equivalent protons [38]. Meanwhile, the isotropic *g* values are very similar for both **TRI-1** and **TRI-2**, measuring 2.0025 and 2.0032, respectively. Consistent with numerous reports, the absence of both the zero-field splitting and the forbidden half-field transition signals primarily results from the highly symmetrical electronic structure of triangulene [41,42]. Both **TRI-1** and **TRI-2** in solid state were stable at room temperature under a nitrogen atmosphere, but they slowly decomposed upon exposure to air. Particularly, **TRI—2** was found to be stable for months in a crystalline state. To deeply understand and compare the stability of **TRI-1** and **TRI-2**, measurements of stability were carried out based on time-dependent UV-vis spectroscopy under ambient atmosphere (Figures 4b and Figure S6). According to the report by Shimizu et al., when a solution of **TRI-1** in CH_2Cl_2 was exposed to air at room temperature, the absorption at 415 nm decreased, and new absorption bands appeared, indicating a slow decomposition with an estimated half-life of approximately 18 h [38]. While the absorption peak at 415 nm of **TRI-2** remained almost unchanged even after 10 h under the same conditions, and based on the decay rate fitting, the half-life of **TRI-2** was estimated to be 132 h. Based on the study reported by Shimizu et al. [38], **TRI-1** exhibited a high sensitivity to air and was prone to oxidation and decomposition. One can expect that when the substituent is replaced with trichlorobenzene, the latter's strong electron-withdrawing characteristics may decrease the oxidation potential of the triangulene fragment, thereby enhancing the oxygen tolerance and overall stability of **TRI-2**. As expected, the cyclic voltammetry and DFT calculations of **TRI-1** and **TRI-2** demonstrate that the trichlorobenzene substituents increase the oxidation potential (E_{ox} = −0.23 V for **TRI-1**, E_{ox} = 0.13 V for **TRI-2**, vs. Fc/Fc^+) and decrease the highest occupied molecular

orbital (HOMO) energy level of the triangulene fragment in comparison to trimethylbenzene substituents (Figure S7). Considering that the aryl groups are perpendicular to the triangulene fragment pi-system, such a distinct substituent effect may be associated with the electronic communication between trichlorobenzene substituents and the triangulene core through inductive and hyperconjugation effects.

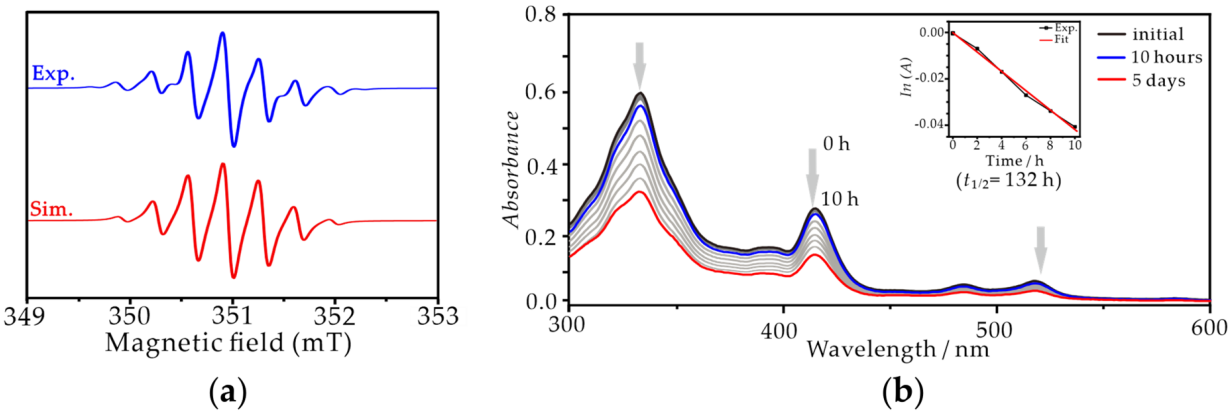


Figure 4. (**a**) X-band EPR spectra of **TRI-2** in toluene (0.5 mM) at 298 K in the dark under a nitrogen atmosphere (blue, experiment; red, simulation). (**b**) The UV-vis absorption spectrum of **TRI-2** over time in toluene (2×10^{-5} M) at 298 K in the dark under ambient atmosphere: 0 h (black line), 10 h later (blue line), and 5 days later (red line) (insert: attenuation of absorption intensity at 415 nm of **TRI-2** over time (dark dotted line) and the fitting line (red line). The half-life of **TRI-2** was roughly estimated to be 132 h (=ln2/−0.005224)).

4. Conclusions

In summary, we have successfully synthesized two kinetically stabilized [3]triangulene derivatives **TRI-1** and **TRI-2** through an oxidative dehydrogenation method. Notably, two distinct isomers of the dihydro-triangulene precursor were thoroughly characterized using UV-vis and NMR spectroscopy, and their structures were unambiguously confirmed by X-ray crystallographic analysis. The electron-rich mesityl groups facilitate the oxidative rearrangement of the triangulene fragment, leading to the formation of the *b*-form isomer **αH-TRI-1**. In contrast, the electron-withdrawing trichlorophenyl groups stabilize the electronic structure of the *a*-form isomer **αH-TRI-2**. This substituent-dependent isomerization underscores the critical role of substituents in modulating the structural and electronic properties of triangulene derivatives. Consequently, the introduction of trichlorophenyl groups significantly enhances the stability of **TRI-2**, e.g., the half-life of **TRI-2** was estimated to be 132 h, which is longer than the half-life of **TRI-1** (18 h). Due to the electron-withdrawing nature of the trichlorobenzene substituent, the oxidation potential of the triangulene fragment may be reduced, thereby enhancing the stability of **TRI-2**. Our novel strategy for synthesizing and stabilizing triangulene not only enables the creation of its high-order analogs but also facilitates the development of open-shell graphene fragments as both solution-processable and solid-state materials.

Supplementary Materials: The following supporting information can be downloaded at https://www.mdpi.com/article/10.3390/chemistry7020039/s1: Figure S1: Consistent with the reported work by Juríček et al, UV-vis spectra recorded during the oxidation process for toluene solutions of a dihydro-precursor **αH-TRI-1** (a) and **αH-TRI-2** (b) with 1 equivalent of DDQ, providing, after 2 h, a mixture of monoradical (red lines in two figures above) and, after 8 h, the triangulene **TRI-1** and **TRI-2** (blue lines in two figures above). The oxidation was performed at a concentration of 2.5 mM. For the UV-vis measurements, an aliquot sample of this solution was diluted to 2×10^{-5} M [37]. Figure S2: Single crystal of **αH-TRI-1**. Figure S3: Single crystal of **αH-TRI-2**. Figure S4: Single crystal

of **TRI-2**. Figure S5: Single crystal packing of **TRI-2** (from left to right: a axis, b axis and c axis). Figure S6: (a) CW X-band EPR spectra of **TRI-1** in toluene (0.5 mM) at 298 K in dark under nitrogen atmosphere (blue, experiment; red, simulation in toluene at 298 K. (b) The attenuation of absorption intensity at 415nm of **TRI-2** over time (dark dot-line) and the fitting line (red line). The half-life of **TRI-2** is roughly estimated to be 132 h (= ln2/−0.005224). (c) The UV-vis absorption spectrum of **TRI-1** and **TRI-2** in toluene (2×10^{-5} M) at 298 K in the dark under ambient atmosphere. Figure S7: (a) Cyclic voltammograms of **TRI-1** and **TRI-2** in CH_2Cl_2 with 0.1 M Bu_4NBF_4 as the supporting electrolyte, Ag/AgCl as the reference electrode, and a Pt wire as the counter electrode and a scan rate at 20 $mV \cdot s^{-1}$. The potential was calibrated against the ferrocenium/ferrocene (Fc^+/Fc) couple. Molecular orbitals of **TRI-1** (b) and **TRI-2** (c) calculated at the TD-UB3LYP/6-31G(d). Figure S8–S33: ^1H NMR and ^{13}C NMR spectra of compounds 2–8. Figure S34: The ^1H NMR spectrum of **αH-TRI-1**. Figure S35: ^1H NMR spectrum of compound **αH-TRI-2** (400 MHz, CD_2Cl_2, 298 K). Table S1: Crystal date of and structure refinement of **αH-TRI-1**. Table S2: Crystal date of and structure refinement of **αH-TRI-2**. Table S3: Crystal date of and structure refinement of **TRI-2**. References [37,43–45] are cited in the Supplementary Materials.

Author Contributions: Conceptualization, methodology, formal analysis, investigation, data curation, Y.Y. and P.L.; writing—original draft preparation, Y.Y.; writing—review and editing, P.L.; visualization, Y.Y.; single crystallographic analysis, X.Z.; supervision, project administration, funding acquisition, X.S. All authors have read and agreed to the published version of the manuscript.

Funding: Shanghai Natural Science Foundation (22ZR1420600).

Data Availability Statement: The original contributions presented in this study are included in the article/Supplementary Materials. Further inquiries can be directed to the corresponding authors.

Acknowledgments: X.S. acknowledges the financial support from the Shanghai Natural Science Foundation (22ZR1420600).

Conflicts of Interest: The authors declare no conflicts of interest.

References

1. Morita, Y.; Suzuki, S.; Sato, K.; Takui, T. Synthetic Organic Spin Chemistry for Structurally Well-Defined Open-Shell Graphene Fragments. *Nat. Chem.* **2011**, *3*, 197–204. [CrossRef] [PubMed]
2. Zeng, W.; Wu, J. Open-Shell Graphene Fragments. *Chem* **2021**, *7*, 358–386. [CrossRef]
3. Liu, J.; Feng, X. Recent Advances in Open-Shell Graphene Fragments. *Angew. Chem. Int. Ed.* **2020**, *59*, 23386–23401. [CrossRef]
4. Morita, Y.; Nishida, S. Phenalenyls, Cyclopentadienyls, and Other Carbon-Centered Radicals. In *Stable Radicals*; Hicks, R.G., Ed.; John Wiley & Sons, Ltd.: Chichester, UK, 2010; Volume 3, pp. 81–145.
5. Han, W.; Kawakami, R.K.; Gmitra, M. Graphene Spintronics. *Nat. Nanotechnol.* **2014**, *9*, 794–807. [CrossRef]
6. Zheng, Y.; Wang, S. Delocalized Magnetism in Low-Dimensional Graphene System. *About Acta Phys. Sin.* **2022**, *71*, 188101. [CrossRef]
7. Yazyev, O.V. Emergence of Magnetism in Graphene Materials and Nanostructures. *Rep. Prog. Phys.* **2010**, *73*, 056501. [CrossRef]
8. Kobayashi, Y.; Fukui, K.; Enoki, T.; Kusakabe, K.; Kaburagi, Y. Observation of Zigzag and Armchair Edges of Graphite Using Scanning Tunneling Microscopy and Spectroscopy. *Phys. Rev. B Condens. Matter Mater. Phys.* **2005**, *71*, 193406. [CrossRef]
9. Philpott, M.R.; Cimpoesu, F.; Kawazoe, Y. Geometry, Bonding and Magnetism in Planar Triangulene Graphene Molecules with D3h Symmetry: Zigzag Cm**2+4m+1H3m+3 (m = 2,· · · , 15). *Chem. Phys.* **2008**, *354*, 1–15. [CrossRef]
10. Bearpark, M.J.; Robb, M.A.; Bernardi, F.; Olivucci, M. Molecular Mechanics Valence Bond Methods for Large Active Spaces. Application to Conjugated Polycyclic Hydrocarbons. *Chem. Phys. Lett.* **1994**, *217*, 513–519. [CrossRef]
11. Das, A.; Müller, T.; Plasser, F.; Lischka, H. Polyradical Character of Triangular Non-Kekulé Structures, Zethrenes, p-Quinodimethane-Linked Bisphenalenyl, and the Clar Goblet in Comparison: An Extended Multireference Study. *J. Phys. Chem. A* **2016**, *120*, 1625–1636. [CrossRef]
12. Pavliček, N.; Mistry, A.; Majzik, Z.; Moll, N.; Meyer, G.; Fox, D.J.; Gross, L. Synthesis and Characterization of Triangulene. *Nat. Nanotechnol.* **2017**, *12*, 308–312. [CrossRef] [PubMed]
13. Sharma, V.; Narayan, S.; Dabhi, S.D.; Jha, P.K. Tailoring the Electronic and Magnetic Properties of Peculiar Triplet Ground State Polybenzoid "Triangulene". *ChemistrySelect* **2018**, *3*, 2390–2397. [CrossRef]

14. Lang, J.; Brabec, J.; Saitow, M.; Pittner, J.; Neese, F.; Demel, O. Perturbative Triples Correction to Domain-Based Local Pair Natural Orbital Variants of Mukherjee's State Specific Coupled Cluster Method. *Phys. Chem. Chem. Phys.* **2019**, *21*, 5022–5038. [CrossRef]
15. Melle-Franco, M. When 1+1 is Odd. *Nat. Nanotechnol.* **2017**, *12*, 292–293. [CrossRef]
16. Ghising, P.; Biswas, C.; Lee, Y.-H. Graphene Spin Valves for Spin Logic Devices. *Adv. Mater.* **2023**, *35*, 2209137. [CrossRef]
17. Song, S.; Su, J.; Telychko, M.; Li, J.; Li, G.; Li, Y.; Su, C.; Wu, J.; Lu, J. On-Surface Synthesis of Graphene Nanostructures with π-Magnetism. *Chem. Soc. Rev.* **2021**, *50*, 3238–3262. [CrossRef]
18. Turco, E.; Mishra, S.; Melidonie, J.; Eimre, K.; Obermann, S.; Pignedoli, C.A.; Fasel, R.; Feng, X.; Ruffieux, P. On-Surface Synthesis and Characterization of Super-nonazethrene. *J. Phys. Chem. Lett.* **2021**, *12*, 8314–8319. [CrossRef]
19. Sil, S.; Santha Bhaskaran, A.; Chakraborty, S.; Singh, B.; Kuniyil, R.; Mandal, S.K. Reduced-Phenalenyl-Based Molecule as a Super Electron Donor for Radical-Mediated C–N Coupling Catalysis at Room Temperature. *J. Am. Chem. Soc.* **2022**, *144*, 22611–22621. [CrossRef]
20. Yang, Y.; Qiu, L.; Shi, X. Chalcogen Effect of Atom Substitution on the Properties of Tris(2,4,6-trichlorophenyl)methyl(TTM) Radical. *Chem. Res. Chin. Univ.* **2023**, *39*, 197–201. [CrossRef]
21. Clar, E.; Stewart, D.G. Aromatic Hydrocarbons. LXV. Triangulene Derivatives. *J. Am. Chem. Soc.* **1953**, *75*, 2667–2672. [CrossRef]
22. Clar, E.; Stewart, D.G. Aromatic Hydrocarbons. LXVIII. Triangulene Derivatives. *J. Am. Chem. Soc.* **1954**, *76*, 3504–3507. [CrossRef]
23. Valenta, L.; Juríček, M. The Taming of Clar's Hydrocarbon. *Chem. Commun.* **2022**, *58*, 10896–10906. [CrossRef] [PubMed]
24. Hara, O.; Tanaka, K.; Yamamoto, K.; Nakazawa, T.; Murata, I. The Chemistry of Phenalenium Systems. XXV the Triangulenyl Dianion. *Tetrahedron Lett.* **1977**, *18*, 2435–2436. [CrossRef]
25. Holt, C.J.; Wentworth, K.J.; Johnson, R.P. A Short and Efficient Synthesis of the [3]Triangulene Ring System. *Angew. Chem. Int. Ed.* **2019**, *58*, 15793–15796. [CrossRef]
26. Ribar, P.; Sŏolomek, T.; Jurícek, M. Gram-Scale Synthesis and Supramolecular Complex of Precursors of Clar's Hydrocarbon Triangulene. *Org. Lett.* **2019**, *21*, 7124–7128. [CrossRef]
27. Allinson, G.; Bushby, R.J.; Paillaud, J.L.; Oduwole, D.; Sales, K. ESR Spectrum of a Stable Triplet π Biradical: Trioxytriangulene. *J. Am. Chem. Soc.* **1993**, *115*, 2062–2064. [CrossRef]
28. Allinson, G.; Bushby, R.J.; Paillaud, J.-L.; Thornton-Pett, M. Synthesis of a Derivative of Triangulene; the First Non-Kekulé Polynuclear Aromatic. *J. Chem. Soc. Perkin Trans.* **1995**, *1*, 385–390. [CrossRef]
29. Allinson, G.; Bushby, R.J.; Jesudason, M.V.; Paillaud, J.-L.; Taylor, N. The Synthesis of Singlet Ground State Derivatives of Non-Kekulé Polynuclear Aromatics. *J. Chem. Soc. Perkin Trans.* **1997**, *2*, 147–156. [CrossRef]
30. Su, J.; Telychko, M.; Song, S.; Lu, J. Triangulenes: From Precursor Design to On-Surface Synthesis and Characterization. *Angew. Chem. Int. Ed.* **2020**, *59*, 7658–7668. [CrossRef]
31. Liu, P.; Wu, M.X.; Yu, M.; Kang, H.; Huang, B.; Yang, H.-B.; Zhao, X.-L.; Shi, X. Synthesis of Polycyclic Aromatic Compounds by Electrocyclization–Dehydrogenation of Diradicaloids. *Org. Lett.* **2024**, *26*, 7914–7919. [CrossRef]
32. Liu, P.; Li, Y.; Wu, M.X.; Kang, H.; Zhao, X.L.; Xu, L.; Liu, L.; Li, X.; Fang, J.; Fang, Z.; et al. Double [5]carbohelicene: Facile synthesis, chiroptical properties, isomerization study, and lasing application. *Sci. China Chem.* **2025**, *68*, 233–240. [CrossRef]
33. Shen, T.; Dijkstra, D.; Farrando-Pérez, A.; Boj, P.G.; Villalvilla, J.M.; Quintana, J.A.; Zou, Y.; Hou, X.; Wei, H.; Li, Z.; et al. Fused Triangulene Dimers: Facile Synthesis by Intramolecular Radical-Radical Coupling and Application for Near-Infrared Lasers. *Angew. Chem. Int. Ed.* **2023**, *62*, e202304197. [CrossRef] [PubMed]
34. Ortiz, R.; Boto, R.A.; García-Martínez, N.; Sancho-García, J.C.; Melle-Franco, M.; Fernández-Rossier, J. Exchange Rules for Diradical π-Conjugated Hydrocarbons. *Nano Lett.* **2019**, *19*, 5991–5997. [CrossRef] [PubMed]
35. Cheng, S.; Xue, Z.; Li, C.; Liu, Y.; Xiang, L.; Ke, Y.; Yan, K.; Wang, S.; Ping, Y. On-Surface Synthesis of Triangulene Trimers via Dehydration Reaction. *Nat. Commun.* **2022**, *13*, 1705. [CrossRef]
36. Inoue, J.; Fukui, K.; Kubo, T.; Nakazawa, S.; Sato, K.; Shiomi, D.; Morita, Y.; Yamamoto, K.; Takui, T.; Nakasuji, K. The First Detection of a Clar's Hydrocarbon, 2,6,10-Tri-tert-butyltriangulene: A Ground-State Triplet of Non-Kekulé Polynuclear Benzenoid Hydrocarbon. *J. Am. Chem. Soc.* **2001**, *123*, 12702–12703. [CrossRef]
37. Valenta, L.; Mayländer, M.; Kappeler, P.; Blacque, O.; Sŏlomek, T.; Richert, S.; Juríček, M. Tri-mesityltriangulene: A Persistent Derivative of Clar's Hydrocarbon. *Chem. Commun.* **2022**, *58*, 3019–3022. [CrossRef]
38. Arikawa, S.; Shimizu, A.; Shiomi, D.; Sato, K.; Shintani, R. Synthesis and Isolation of a Kinetically Stabilized Crystalline Triangulene. *J. Am. Chem. Soc.* **2021**, *143*, 19599–19605. [CrossRef]
39. Zhang, F.; Hong, K.; Li, T.; Park, H.; Yu, J. Functionalization of C(sp^3)–H Bonds Using a Transient Directing Group. *Science* **2016**, *351*, 252–256. [CrossRef]
40. Gu, Y.; Wu, X.; Gopalakrishna, T.Y.; Phan, H.; Wu, J. Graphene-like Molecules with Four Zigzag Edges. *Angew. Chem. Int. Ed.* **2018**, *57*, 6541–6545. [CrossRef]
41. Turco, E.; Bernhardt, A.; Krane, N.; Valenta, L.; Fasel, R.; Juríček, M.; Ruffieux, P. Observation of the magnetic ground state ofthe two smallest triangular nanographenes. *JACS Au* **2023**, *3*, 1358–1364. [CrossRef]

42. Yu, H.; Heine, T. Magnetic Coupling Control in Triangulene Dimers. *J. Am. Chem. Soc.* **2023**, *145*, 19303–19311. [CrossRef] [PubMed]
43. Mallory, F.B.; Butler, K.E.; Bérubé, A.; Luzik, E.D.; Mallory, C.W.; Brondyke, E.J.; Hiremath, R.; Ngo, P.; Carroll, P.J. Phenacenes: A family of graphite ribbons. Part 3: Iterative strategies for the synthesis of large phenacenes. *Tetrahedron* **2001**, *57*, 3715–3724. [CrossRef]
44. Umemoto, T.; Singh, R.P.; Xu, Y.; Saito, N. Discovery of 4-tert-Butyl-2,6-dimethylphenylsulfur Trifluoride as a Deoxofluorinating Agent with High Thermal Stability as Well as Unusual Resistance to Aqueous Hydrolysis, and Its Diverse Fluorination Capabilities Including Deoxofluoro-Arylsulfinylation with High Stereoselectivity. *J. Am. Chem. Soc.* **2010**, *132*, 18199–18205. [PubMed]
45. Tian, Y.; Uchida, K.; Kurata, H.; Hirao, Y.; Nishiuchi, T.; Kubo, T. Design and Synthesis of New Stable Fluorenyl-Based Radicals. *J. Am. Chem. Soc.* **2014**, *136*, 12784–12793. [CrossRef]

Disclaimer/Publisher's Note: The statements, opinions and data contained in all publications are solely those of the individual author(s) and contributor(s) and not of MDPI and/or the editor(s). MDPI and/or the editor(s) disclaim responsibility for any injury to people or property resulting from any ideas, methods, instructions or products referred to in the content.